

# Well-Defined Mesostructured Organic–Inorganic Hybrid Materials via Atom Transfer Radical Grafting of Oligomethacrylates onto SBA-15 Pore Surfaces

J. Moreno<sup>\*,†</sup> and D. C. Sherrington<sup>‡</sup>

Department of Chemical and Environmental Technology, ESCET, Universidad Rey Juan Carlos, Móstoles, Spain and WestChem Graduate School of Chemistry, Department of Pure and Applied Chemistry, University of Strathclyde, Glasgow, United Kingdom

Received December 4, 2007. Revised Manuscript Received April 25, 2008. Accepted April 29, 2008

Well-ordered mesoporous organic–inorganic hybrid materials based on ATRP of methacrylate monomers inside SBA-15 pores have been synthesized maintaining the mesoporosity. Initially SBA-15 materials were functionalized with the ATRP initiator by reaction of surface hydroxyl groups with (3-aminopropyl)-triethoxysilane (APTES) and 2-bromo-2-methylpropionyl bromide (BMPB); thus growth of oligomethacrylates occurred directly from the mesoporous walls. Two methacrylate monomers (MMA and GMA) and different monomer/initiator molar ratios (5/1 – 25/1) were tested. The characterization of the hybrid materials included N<sub>2</sub> adsorption–desorption porosimetry, X-ray diffraction, <sup>29</sup>Si MAS NMR, FT-IR spectroscopy, TEM and TG analysis. The results show that mesostructured hybrid materials with grafted oligomethacrylates maintain good porosity (~ 0.4 cm<sup>3</sup>/g) and BET surface area (~ 300 m<sup>2</sup>/g) with potential for use as catalyst components in chemical processes. The grafting of GMA-based oligomers is particularly important because the epoxide functionality allows further facile and versatile chemical modification, for example to introduce particular ligand structures and thence specific metal complexes.

## Introduction

Functionalization of mesostructured silicas (such as MCM-41 or SBA-15) has attracted considerable research interest in the past few years.<sup>1</sup> In this context, the covering of a silica surface with different polymers seems to be a potentially useful strategy for incorporating a range of organic functional groups which could modify the properties of these materials and open up new fields for novel applications. Many previously published investigations have reported on the preparation of organic–inorganic hybrid materials by polymerization of different monomers inside silica channels or around silica particles. For example, Moller et al. describe the incorporation of methacrylate groups (MMA) into MCM-41 walls through co-condensation of tetramethoxysilane and 3-(trimethoxysilyl)propyl methacrylate resulting in reactive hybrid materials;<sup>2</sup> after polymerization of these inner pore methacrylate groups with adsorbed MMA a new composite organic–inorganic hybrid material is obtained. Von Werne et al. report the synthesis of structurally well-defined polymer–nanoparticle hybrids by atom transfer radical polymerization (ATRP) of styrene over silica particles functionalized with the ATRP initiator.<sup>3,4</sup> Choi et al. investigate free-radical polymerization of several vinyl monomers inside SBA-15 mesoporous; they observed that

the silica structure and polymerization conditions can alter the structure of the polymers obtained and, therefore, the adsorption properties of the hybrid materials.<sup>5</sup> Save et al. describe the preparation of hybrid materials via ATRP of styrene and methyl methacrylate inside pores of a MSU ordered silica, decreasing the BET surface area down to 35 m<sup>2</sup>/g and the total pore volume from 1.53 to 0.053 cm<sup>3</sup>/g.<sup>6</sup> Fu et al. detail the design, synthesis, and characterization of silica with a well-defined porous network in which the size and surface of the pores is modified by ATRP of *N*-isopropyl acrylamide.<sup>7</sup>

According to the literature, two main difficulties are encountered during the functionalization of a mesoporous silica with a covering of polymer. The first one is to get polymers covalently linked to the inorganic materials. Different strategies have been tested to achieve this aim, such as polymerization of monomers included in the silica walls by co-condensations<sup>2</sup> or grafting of polymerization initiator over the silica surface to induce polymer growth only from inorganic walls.<sup>3,4,6–9</sup> The second difficulty in this kind of functionalization process is to avoid destroying the silica pore system by infilling with excess polymer. In this context, ATRP based on reversible termination could be a very useful

\* To whom the correspondence should be addressed. Phone: 34-91-4888087. Fax: 34-91-4887068. E-mail: jovita.moreno@urjc.es.

<sup>†</sup> Universidad Rey Juan Carlos.

<sup>‡</sup> University of Strathclyde.

(1) Wight, A. P.; Davis, M. E. *Chem. Rev.* **2002**, *102*, 3589.

(2) Moller, K.; Bein, T.; Fisher, R. X. *Chem. Mater.* **1999**, *11*, 665.

(3) von Werne, T.; Patten, T. E. *J. Am. Chem. Soc.* **1999**, *121*, 7409.

(4) von Werne, T.; Patten, T. E. *J. Am. Chem. Soc.* **2001**, *123*, 7497.

(5) Choi, M.; Kleitz, F.; Liu, D.; Lee, H. Y.; Ahn, W.-S.; Ryo, R. *J. Am. Chem. Soc.* **2005**, *127*, 1924.

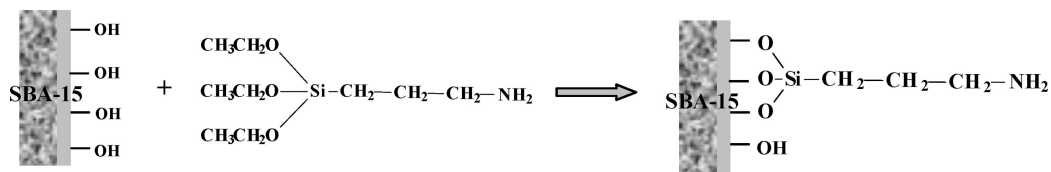
(6) Save, M.; Granvorka, G.; Bernard, J.; Charleux, B.; Boissière, C.; Grosso, D.; Sanchez, C. *Macromol. Rapid Commun.* **2006**, *27*, 393.

(7) Fu, A.; Rama Rao, G. V.; Ista, L. K.; Wu, Y.; Andrzejewski, B. P.; Sklar, L. A.; Ward, T. L.; López, G. P. *Adv. Mater.* **2003**, *15*, 1262.

(8) Perruchot, C.; Khan, M. A.; Kamitsi, A.; Armes, S. P. *Langmuir* **2001**, *17*, 4479.

(9) Kruk, M.; Dufour, B.; Celer, E. B.; Kowalewski, T.; Jaroniec, M.; Matyjaszewski, K. *J. Phys. Chem. B* **2005**, *109*, 9216.

Scheme 1. Chemical Attachment of Aminopropyl Groups



Scheme 2. Reaction between Amino Groups and BMPB and Attachment of the ATRP Initiator

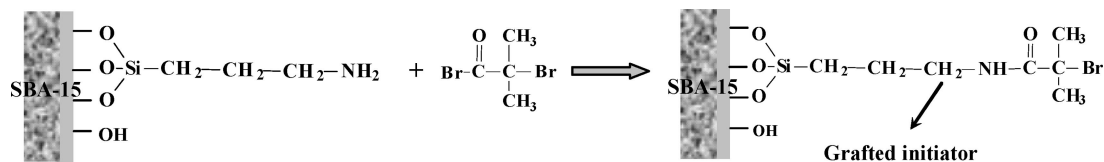


Table 1. Physicochemical Properties of the Materials under Study

sample	description	microanalysis, % C	$S_{\text{BET}}^a$ ( $\text{m}^2/\text{g}$ )	$\text{N}_2$ adsorption–desorption				XRD	
				$D_{\text{pore}}^b$ (nm)	$V_{\text{pore}}^c$ ( $\text{cm}^3/\text{g}$ )	$V_{\text{meso}}^d$ ( $\text{cm}^3/\text{g}$ )	$V_{\text{micro}}^e$ ( $\text{cm}^3/\text{g}$ )	$d(100)$ (nm)	wall <sup>f</sup> thickness (nm)
SBA-15	initial support	0.3	782	8.2	1.12	0.74	0.097	9.3	2.5
SBAIn1	SBA + initiator 1 (1.6 mmol $\text{NH}_2/\text{g}$ )	13.7	305	6.5	0.50	0.36	0.008	9.5	4.5
In1MMAi	MMA polymerization using $M/I = 10$	25.3	76	5.5	0.13	0.06	0.002	9.5	5.5
In1MMAii	MMA polymerization using $M/I = 5$	19.1	250	6.0	0.39	0.27	0.005	9.6	5.1
SBAIn2	SBA + initiator 2 (1.0 mmol $\text{NH}_2/\text{g}$ )	7.3	358	6.8	0.65	0.41	0.016	9.4	4.1
In2MMA	MMA polymerization using $M/I = 10$	10.1	285	6.7	0.46	0.32	0.008	9.9	4.7
In2GMAi	GMA polymerization using $M/I = 10$	11.8	302	6.1	0.47	0.32	0.008	9.8	5.2
In2GMAii	GMA polymerization using $M/I = 25$	13.4	224	6.0	0.34	0.24	0.006	9.6	5.1

<sup>a</sup> BET specific surface area. <sup>b</sup> Mesoporous surface area calculated by the  $t$ -plot method. <sup>c</sup> Total pore volume calculated by the BJH method. <sup>d</sup> Mesoporous pore volume calculated by the  $t$ -plot method. <sup>e</sup> Microporous pore volume calculated by the  $t$ -plot method. <sup>f</sup> Calculated by  $a_0$  – BJH pore size ( $a_0 = 2d(100)/\sqrt{3}$ ).

tool for maintaining the mesoporosity in silica since this technique allows better control over the molecular weight, molecular weight distribution, and structure of the polymer obtained.<sup>6–9</sup>

Here, we report a procedure to synthesize well-ordered mesoporous organic–inorganic hybrid materials based on ATRP of methacrylate monomers inside SBA-15 pores while maintaining the system's porosity. The ATRP initiator is chemically bound to the mesostructure walls beforehand such that polymer growth occurs directly from and over the SBA-15 internal surface. The developed procedure now provides an opportunity for incorporation of numerous functional groups while retaining the important properties (narrow pore size distribution, high pore size, and high surface area) of mesostructured materials.

## 2. Experimental Section

**2.1. Synthesis of SBA-15 Materials.** SBA-15 material was synthesized according to the procedure reported by Zhao et al.<sup>10</sup> using Pluronic 123 triblock copolymer ( $\text{EO}_{20}\text{-PO}_{70}\text{-EO}_{20}$ ; Aldrich) as a template. In a typical synthesis 4 g of Pluronic 123 was dissolved under stirring in 125 mg of 1.9 M HCl at room temperature. The solution was heated to 40 °C before adding

tetraethylorthosilicate (TEOS; Aldrich). The resultant solution was stirred for 20 h at 40 °C, followed by aging at 110 °C for 24 h under static conditions. The solid product was recovered by filtration and dried at room temperature overnight. The template was removed from the as-made mesoporous material by calcination at 550 °C for 5 h (heating rate = 1.8 °C  $\text{min}^{-1}$ ).

**2.2. Attachment of the ATRP Initiator.** Attachment of the initiator was carried out by two successive reactions on the calcined SBA-15 material previously outgassed under vacuum at 40 °C overnight. In the first reaction, outgassed SBA-15 material was introduced into a round-bottomed flask containing 200 mL of dry toluene and the required amount of (3-aminopropyl)triethoxysilane (APTES, Aldrich). The mixture was stirred for 5 h under reflux and a nitrogen atmosphere. Under these conditions, the hydroxyl groups of the SBA-15 surface react with the ethoxy groups of the APTES molecules, leading an amino-functionalized SBA-15 material (Scheme 1). After reaction, the solid was recovered by filtration and intensively washed with toluene in a Soxhlet apparatus. Finally, before the next reaction, the solid was outgassed again under vacuum at 40 °C.

In the second reaction, 2-bromo-2-methylpropionyl bromide (BMPB, Aldrich) was used to react with the previously attached aminopropyl groups leading the ATRP initiator bonded on SBA-15 pores surface (Scheme 2). In this case, functionalized SBA-15 material was added to 200 mL of dry dichloromethane and stirred for 3 h under reflux and a nitrogen atmosphere. Triethylamine (Aldrich) was employed as the basic catalyst, and BMPB/aminopropyl and triethylamine/aminopropyl molar ratios were 1.5 and 2, respectively. Finally, the solid

(10) Zhao, D.; Feng, J.; Huo, Q.; Melosh, N.; Fredrickson, G. H.; Chmelka, B. F.; Stucky, G. D. *Science* **1998**, 279, 548.

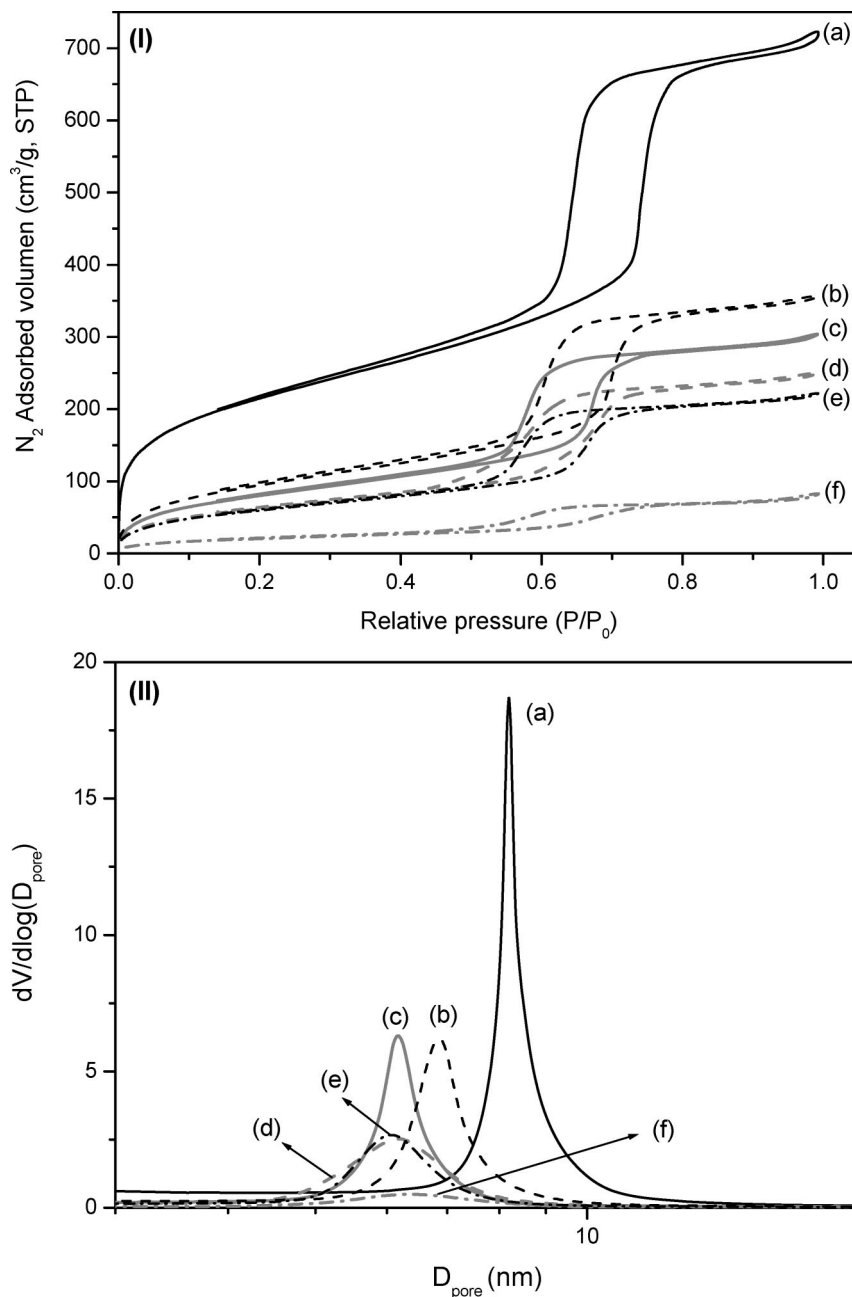


**Figure 1.** N<sub>2</sub> adsorption–desorption isotherms (I) and pore size distributions (II) of the materials under study: SBA-15 (a), SBAIn2 (b), In2GMAi (c), In1MMAii (d), In2GMAii (e), and In1MMAi (f).

was also recovered by filtration, washed with toluene, and outgassed under vacuum at 40 °C overnight.

**2.3. Methyl Methacrylate (MMA) and Glycidyl Methacrylate (GMA) Oligomerization.** In a typical reaction, 0.3 g of SBA-15 functionalized with the ATRP initiator was mixed with 3 mL of dry toluene in a test tube. Then, copper(I) chloride (CuCl, Aldrich) and 2,2'-bipyridyl (Bipy, Aldrich) were added using an initiator/CuCl/Bipy molar ratio of 1/1/3. Next, the necessary amount of methacrylate monomer (methyl methacrylate or glycidyl methacrylate, Aldrich) in order to limit the DP<sub>N</sub> of the chains formed to ~5–25 was added to the mixture (e.g., DP<sub>N</sub> = 10 requires mol<sub>MMA</sub>/mol<sub>init</sub> = 10; hence, mass<sub>MMA</sub> = mole initiator g<sup>-1</sup> SBA-15 × 10 × 100.12 × 0.3). The test tube was then filled with nitrogen, hermetically closed, and stirred for 15 h at 60 °C. After polymerization, the solid was recovered by filtration, washed with toluene using a Soxhlet extractor, and outgassed under vacuum at 40 °C for 24 h in order to remove the volatiles from the porous system.

**2.4. Hybrid Materials Characterization.** The carbon and nitrogen contents of the hybrid materials were determined by elemental microanalyses carried out on a Perkin-Elmer 2400 analyzer by the Elemental Microanalytical Service available within the Department of Pure and Applied Chemistry at the University of Strathclyde. Nitrogen adsorption–desorption isotherms at 77 K were obtained with a Micromeritics ASAP 2000 apparatus. The samples were previously outgassed under vacuum at 50 °C overnight. Surface areas were calculated using the BET equation, whereas pore size distributions were determined by the BJH method applied to the adsorption branch of the isotherms. Mean pore size was obtained from the maximum of BJH pore size distribution. Low-angle XRD patterns (0.6° < 2θ < 5°) were acquired on a Philips X'PERT MPD diffractometer using Cu Kα radiation with a step size of 0.02° and a counting time of 5 s. Fourier transform IR (FT-IR) spectra of hybrid materials were recorded on a Perkin-Elmer 1600 series FTIR instrument using the potassium bromide

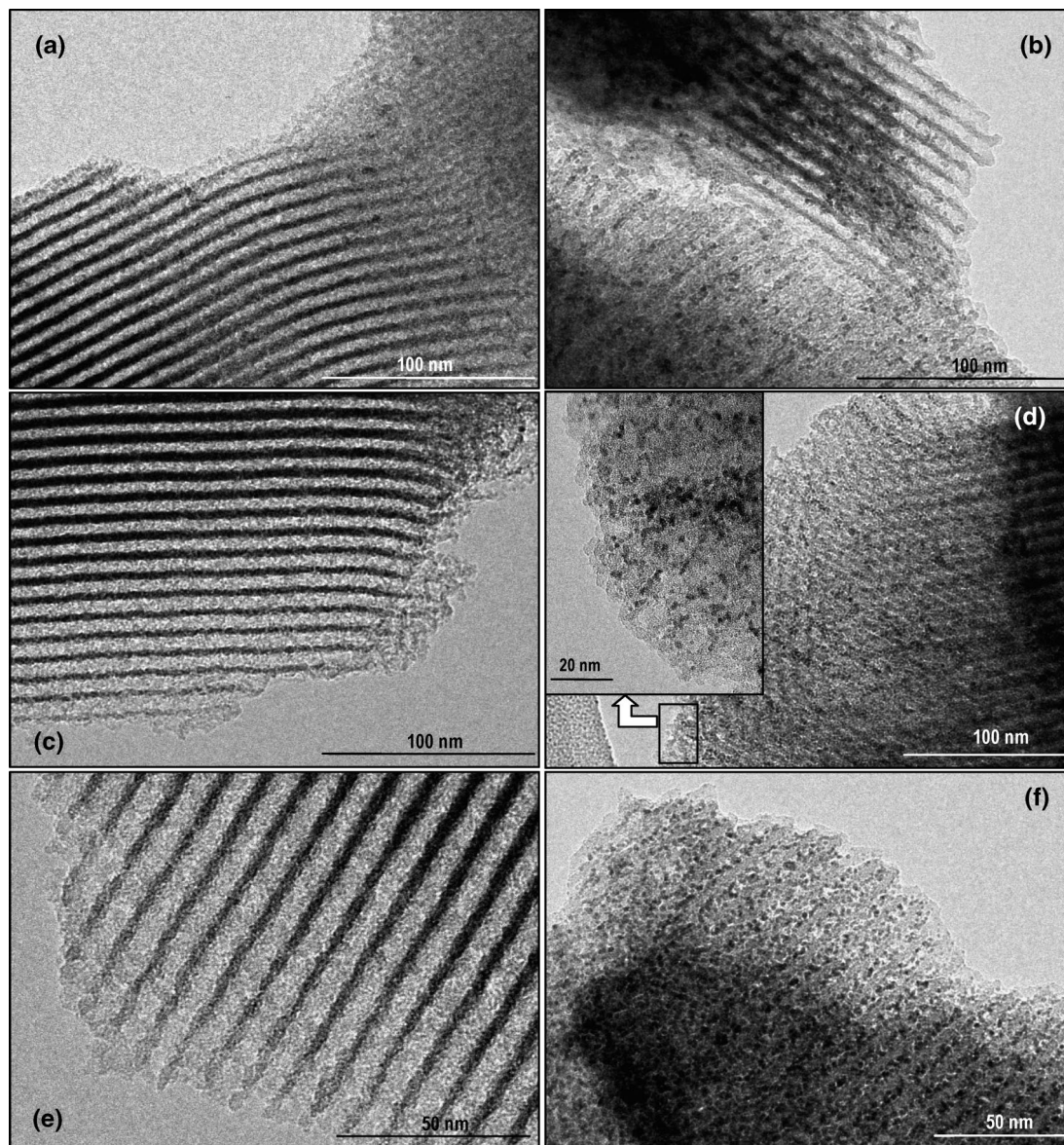


**Figure 2.** TEM micrographs of several samples: stained SBA-15 (a), stained SBAIn1 (b), In1MMAii (c), stained In1MMAii (d), In2GMAii (e), and stained In2GMAii (f).

plates. Thermogravimetric measurements (TGA) were performed in air flow on a TA instrument SDT 2960 thermobalance with a heating rate of 5 °C/min up to 700 °C. Transmission electron micrographs (TEM) were recorded using a 200 kV Philips Tecnai 20 electron microscope. Before TEM analysis, some samples were treated with RuO<sub>4</sub> vapor for 15 min in order to stain the organic species and hence locate the initiator and grafted oligomers on the SBA-15 surface.<sup>11,12</sup> Solid-state <sup>29</sup>Si NMR experiments were performed on a VARIAN-Infinity 400 spectrometer operating at a frequency of 79.4 MHz with the following conditions: magic-angle spinning at 6 kHz;  $\pi/2$  pulse, 4.5  $\mu$ s; a repetition delay of 15 s; and 3000 scans. Spectra were referenced to tetramethylsilane.

### 3. Results and Discussion

Table 1 summarizes the physicochemical properties of several hybrid materials prepared using methyl methacrylate (MMA) or glycidyl methacrylate (GMA) with monomer/initiator (M/I) molar ratios of 5/1–25/1. The properties of the precursor and functionalized SBA-15 materials are also shown for comparison purposes. It can be seen that attachment of the initiator to the

SBA-15 surface leads to a significant reduction of pore size, pore volume, and surface area. This fall in overall porosity is reduced when the quantity of initiator attached is reduced (i.e., the porosity of SBAIn2 is higher than that of SBAIn1). Regarding the properties of hybrid materials themselves, we observe that sample In1MMAi has very low porosity whereas its carbon content is the highest. In this case, it seems there was too much monomer in the polymerization medium, and thus, the porous system of SBAIn1 has become almost completely filled with polymer. In order to prepare hybrid materials retaining higher porosities, two alternatives were explored: (1) decreasing the quantity of monomer (M/I = 5) used during the polymerization reaction, i.e., sample In1MMAii, and (2) reducing the level of initiator attached to the SBA-15 surface, i.e., preparation of sample SBAIn2. The new materials obtained, In1MMAii, In2MMA, In2GMAi, and In2GMAii, all show pore sizes, pore volumes, and surface areas slightly lower than their corresponding precursor materials, but they all retain most of their mesoporosity and hence their potential value as

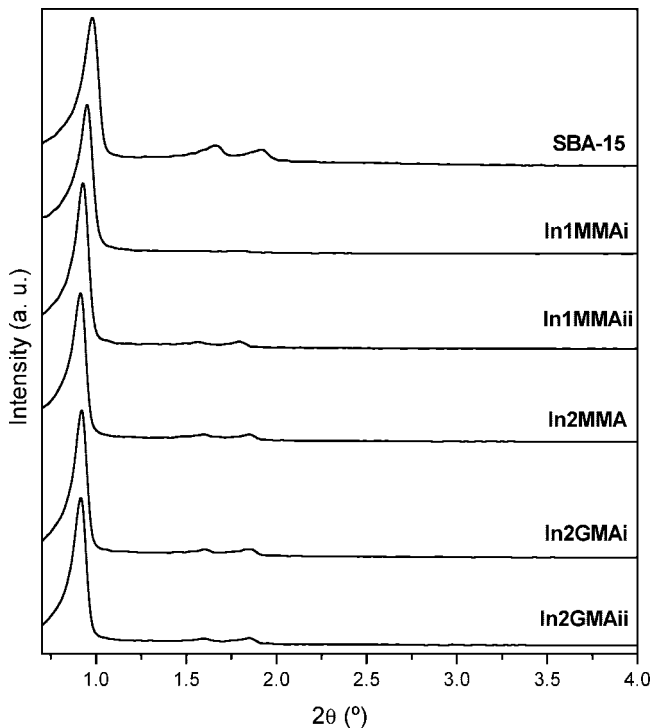


Figure 3. X-ray patterns of the materials under study.

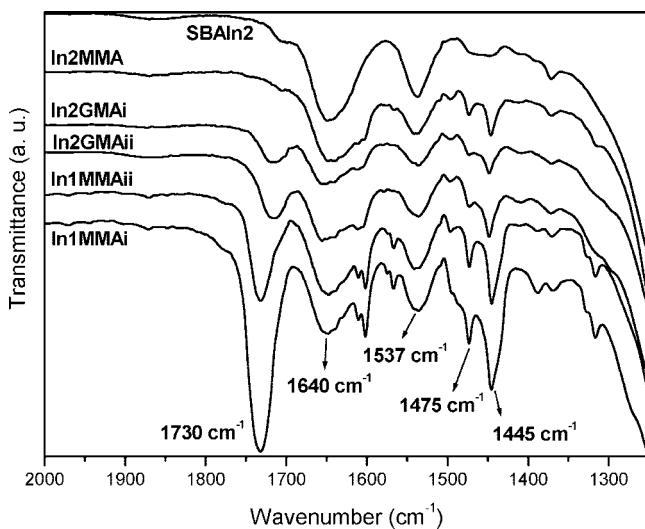


Figure 4. FTIR spectra of the materials under study.

heterogeneous supports in numerous processes. These results contrast with those presented in a previous work by Save et al. where, after MMA polymerization inside the pores of a MSU ordered mesoporous silica, the porosity is fully lost.<sup>6</sup>

Table 1 displays the pore volume corresponding to the mesopores and micropores which have been calculated by means of the *t*-plot method.<sup>13</sup> The data show that surface attachment of initiator and oligomeric methacrylates does not change significantly the mesopore fraction contribution to the total pore volume. However, the micropore fraction contribution is significantly reduced in the hybrid materials. We think that

this reduction can be caused by two factors: on one hand, the surface grafting of the initiator and subsequent monomer–oligomerization can produce some micropore filling and, on the other hand, the presence of oligomethacrylates in the mesopores hinders access to the micropores since the latter are accessed primarily from the mesopores and only to a small extent from the external surface.

The shape of N<sub>2</sub> adsorption–desorption isotherms of hybrid materials allows discrimination between uniformly coated cylindrical pores or blocked pores. Figure 1I shows the N<sub>2</sub> adsorption–desorption isotherms of the materials under study. It can be observed that the precursor SBA-15 presents a clear H1-type hysteresis loop at high relative values, typical for this kind of mesostructured materials. Incorporation of the polymerization initiator (sample SBAIn2, line b) produces a reduction of pore volume and BET area, but the isotherm obtained displays a similar shape to that of the SBA-15 isotherm. After MMA and GMA polymerization (samples In2GMAi, In1MMAii, In2GMAii, and In1MMAi, lines c, d, e, and f, respectively), a decrease of the isotherms vertical position is observed with increasing organic content for each monomer. This trend can also be seen in the pore size distributions of the materials which are presented in Figure 1II. The comparison between In1MMAii (line d) and In1MMAi (line f) distributions indicate that the higher carbon content leads to a less homogeneous pore size. A similar trend is also observed when comparing the distributions of In2GMAi and In2GMAii (lines c and e, respectively). In conclusion, the N<sub>2</sub> adsorption–desorption isotherms and pore size distributions show that a good oligomer distribution inside SBA-15 pores has been achieved for In2GMAi, In1MMAii, and In2GMAii samples, leading to uniformly coated systems.

The distribution of the organic phase inside the SBA-15 porous system was also studied by transmission electron microscopy. Since the low atomic weight of carbon in comparison with silicon makes detection of the initiator and oligomers inside SBA-15 pores difficult by conventional TEM analysis, RuO<sub>4</sub> was used as a staining agent. Addition of heavy atoms to specific structures often provides enough contrast to observe polymers by TEM.<sup>11,12</sup> This staining technique was used with the SBA-15, SBAIn1, In1MMAii, and In2GMAii materials, and TEM micrographs were taken before and after RuO<sub>4</sub> application. These images are presented in Figure 2, where well-ordered hexagonal arrays of 1D mesoporous channels can be observed for hybrid materials, showing a 2D *P6mm* hexagonal structure, typical for SBA-15 solids.<sup>10</sup> In addition, the TEM micrographs also show that staining of the SBAIn1 sample with RuO<sub>4</sub> (Figure 2b) leads to little dark areas which are not observed after staining of SBA-15 (Figure 2a). These results indicate that an interaction between RuO<sub>4</sub> and the amide groups of the ATRP initiator has occurred,<sup>11,12</sup> and they show that the initiator molecules are well dispersed over the silica surface. The stained areas are also observed in the In1MMAii sample after treatment with RuO<sub>4</sub> (Figure 2d), whereas typical pore channels are detected before the staining process (Figure 2c). It is noticeable that the TEM micrographs of stained SBAIn1

(11) Sawyer, L. C.; Grubb, D. T. *Polymer Microscopy*; Chapman & Hall: London, 1996; pp 102–122

(12) Sanz, R.; Calleja, G.; Arencibia, A.; Sanz, E. *Advanced micro- and mesoporous materials, Book of Abstracts, Second International Symposium: Varna, 2007*; pp 108–109.

(13) van Grieken, R.; Calleja, G.; Stucky, G. D.; Melero, J. A.; Garcia, R. A.; Iglesias, J. *Langmuir* **2003**, *19*, 3966.

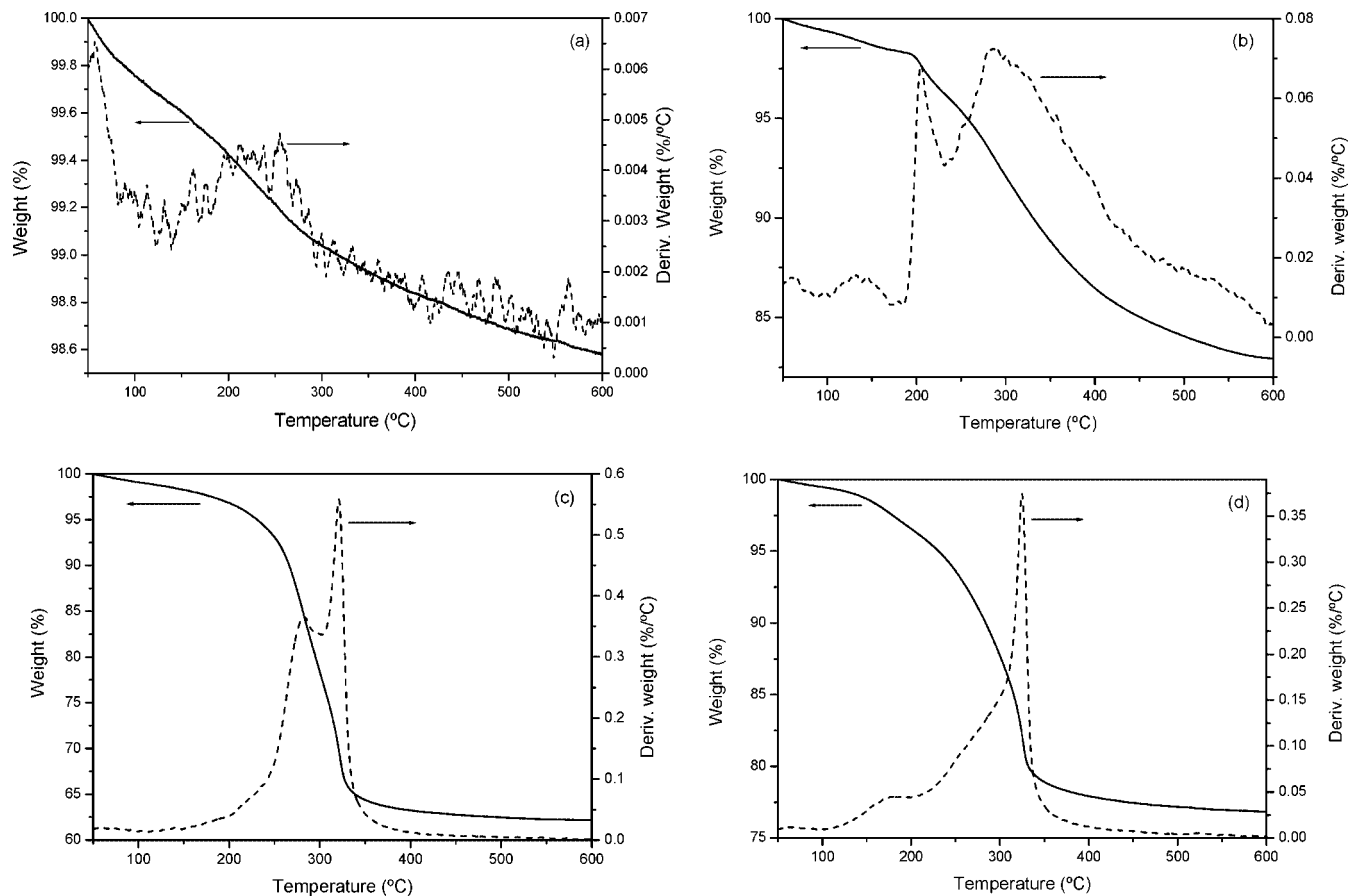


Figure 5. TG analysis of several samples: calcined SBA-15 (a), SBAIn2 (b), In1MMAii (c), and In2GMAii (d).

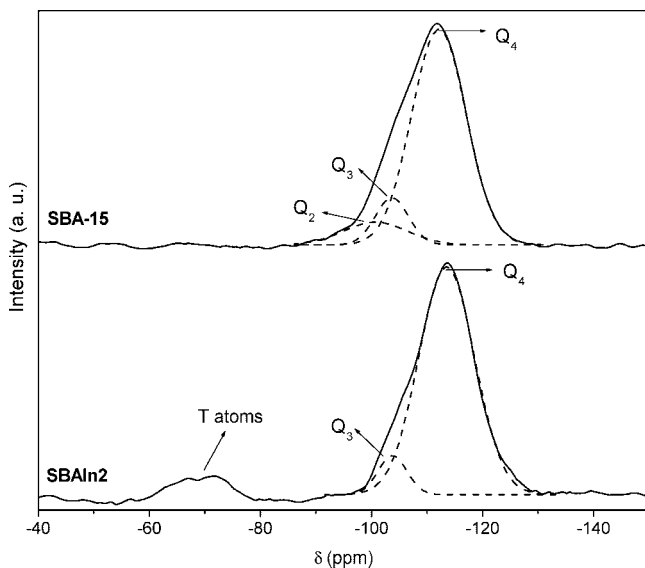


Figure 6.  $^{29}\text{Si}$  MAS NMR spectra of SBA-15 and SBAIn2 materials.

and In1MMAii samples are similar (Figures 2b and 2d) in that in both cases well-dispersed nonorientated dark areas are observed. This could indicate that the interaction between the grafted PMMA and  $\text{RuO}_4$  is rather weak. In contrast, all the channels of the stained sample of In2GMAii seem to be almost filled with dark areas very closely packed together and orientated along the channels (Figure 2f), and this feature is not observed in the same material before  $\text{RuO}_4$  application (Figure 2e). Thus, it is possible that the interaction between  $\text{RuO}_4$  and PGMA is much stronger than that between  $\text{RuO}_4$

and PMMA and increases the density of the organic phase, thus enhancing the contrast and showing the location of the polymer more clearly inside the SBA-15 pores.<sup>11</sup> In conclusion,  $\text{N}_2$  adsorption–desorption isotherms and TEM micrographs of hybrid materials show evidence of a well-distributed and ordered organic phase inside SBA-15 pores.

Although the hexagonal structure of hybrid materials has been previously observed by TEM, this mesoscopic ordering was also evaluated by low-angle X-ray diffraction. Figure 3 shows the X-ray diffraction patterns of the hybrid materials and parent SBA-15 support. The results indicate that the hybrid materials maintain the hexagonal symmetry typical of SBA-15 solids since well-resolved peaks ascribed to the (100), (110), and (200) planes are observed in almost all cases. The XRD pattern of In1MMAi shows lower intensities of the (110) and (200) peaks relative to the (100) peak compared to those obtained for the other hybrid materials. Some authors relate these relative intensity variations to changes in the ratio between material wall thickness and pore size.<sup>14</sup> This explanation seems to be reasonable in this case since In1MMAi is the hybrid material with the largest wall thickness and lowest pore size. Table 1 summarizes the  $d(100)$  and wall thickness values for the materials under study. The slight changes observed in the  $d(100)$  parameter do not seem to indicate any change of silica mesostructure. All the changes recorded are smaller than 7%, and thus, we believe that this does not represent clear evidence indicative of any change of silica mesostructure. Evidently, the

(14) Sauer, J.; Marlow, F.; Schüth, F. *Phys. Chem. Chem. Phys.* **2001**, *3*, 5579.

decrease of the pore size associated with attachment of the initiator and the graft oligomerizations involve an increase of the pore wall thickness.

FTIR spectroscopy was employed to study the presence of organic species associated with the SBA-15 material after initiator grafting and methacrylate oligomerization. Figure 4 shows the FTIR spectra of the materials under study centered on the C=O vibration region. The principal bands observed in all the spectra correspond to water retained by siliceous materials ( $1640\text{ cm}^{-1}$ ), the amide C=O group of the initiator ( $1537\text{ cm}^{-1}$ ), and  $-\text{CH}_3$  and  $-\text{CH}_2$  groups of the initiator and/or of the oligomers ( $1475$  and  $1445\text{ cm}^{-1}$ ).<sup>15</sup> Additionally, samples In1MMAi, In1MMAii, In2GMAi, and In2GMAii show an important band around  $1720\text{--}1730\text{ cm}^{-1}$  associated with the presence of the ester C=O groups of the grafted oligomers.<sup>15</sup> This confirms the effectiveness of the grafting, and indeed, the intensity of this band seems to correlate well with the relative feed level of each monomer employed (Figure 4) and the resulting % carbon detected in each hybrid material (Table 1). The maximum intensity is seen in the spectrum of In1MMAi, which has the highest % carbon and the lowest porosity features, whereas the band in the spectrum of In2MMA is very weak and the % carbon is the lowest of all. Indeed, in this material the level of grafting achieved seems to be very low.

Thermogravimetric analysis of hybrid materials was used to confirm the organic content of the samples and evaluate their thermal stability under an oxidizing atmosphere. Figure 5 displays the TG analyses of the calcined SBA-15 support and hybrid materials obtained under air flow. Calcined SBA-15 material displays a total weight loss lower than 1.5% relative to elimination of retained water and surface dehydroxylation. Thermal decomposition of the SBAIn2 sample (Figure 5b) shows two main weight loss steps around 203 and 289 °C. The first step could be related to elimination of the bromide centers since the C–Br bond is the weakest bond existing in the initiator molecule. Then, the second step might correspond to decomposition of the rest of the initiator. Regarding the thermal decomposition of materials after methacrylate polymerization (In1MMAii, Figure 5c, and In2GMAii, Figure 5d) it can be seen that decomposition of both grafted oligomers occurs in two main steps with rate maxima at 281 and 320 °C for PMMA and 273 and 326 °C for PGMA. Similar thermal degradation behaviors have been previously reported for these polymers.<sup>16,17</sup> Typically, the peak at lower temperature is associated with degradation of the vinyl-terminated chains. For all the materials the organic contents quantified by TG analysis are in agreement with data obtained from elemental microanalysis.

Finally, hybrid materials were analyzed by <sup>29</sup>Si MAS NMR in order to verify that the initiator and therefore the oligomers

are covalently bonded to the SBA-15 walls. As Figure 6 shows, the precursor SBA-15 material shows only one broad band which can be deconvoluted to obtain three signals located at  $-112$  ( $Q_4$  species),  $-104$  ( $Q_3$  species), and  $-99$  ppm ( $Q_2$  species).<sup>18</sup> Attachment of the initiator leads to a decrease of the  $Q_3$  and  $Q_2$  species, whereas a broad new signal is detected around  $-70$  ppm. This resonance is assigned to T silicon species<sup>18</sup> and indicates that some hydroxyl groups, initially at the  $Q_2$  and  $Q_3$  silicon atoms, have reacted with APTES molecules to covalently attach the amine functionality. Similar quantities of T atoms and nitrogen were detected in the materials by means of <sup>29</sup>Si MAS NMR spectra and microanalysis, indicating that the reaction indeed has taken place in the expected way. Furthermore, since the same amount of nitrogen and bromide was observed in the SBAIn1 and SBAIn2 samples ( $\sim 1.6$  and  $1.0$  mmol/g, respectively) it follows that all aminopropyl groups were converted into initiator species. After grafting of the oligomers no significant changes in the distribution of silicon species was noticed. This confirms that interaction between the oligomers and the silica surface occurs via the initiator linkage.

#### 4. Conclusions

The results obtained show that well-defined hybrid materials can be easily synthesized by attachment of an ATRP initiator to the internal surface of SBA-15 and subsequent graft oligomerization of methacrylate monomers. Appropriate adjustment of the reaction conditions of the grafting process allows generation of hybrid materials that maintain the best properties of the two components, i.e., the mesoscopic ordering and porosity of the SBA-15 structure and the organic functionality delivered by the oligomers. Nitrogen physisorption and TEM images indicate that organic phase is uniformly distributed inside the SBA-15 pore system, leading to materials with enough porosity to be used in numerous chemical processes. The XRD patterns of the hybrid materials are characteristic of well-ordered solids with the typical SBA-15 hexagonal symmetry. FTIR spectroscopy and TG analysis confirm the effectiveness of grafting of the methacrylate oligomers and show a clear correlation between the relative feed level of each monomer employed and the resulting % carbon detected in each hybrid material. <sup>29</sup>Si MAS NMR spectroscopy also seems to verify that the initiator and therefore oligomers are covalently bonded to the SBA-15 walls.

Grafting of GMA-based oligomers is particularly important because the epoxide functionality will allow further facile and versatile chemical modification, for example, to introduce particular ligand structures<sup>19</sup> and hence specific metal complexes. We are currently exploring these possibilities. In effect the present approach seems to offer a convenient route to reactive mesostructured polymer-based materials and applications involving such species.

CM703436N

(15) Ning, Y.-C. *Structural Identification of Organic Compounds with Spectroscopic Techniques*; Wiley-VCH: Weinheim, 2005; pp 437–447.

(16) Manring, L. E. *Macromolecules* **1988**, *21*, 530.

(17) Ji, G.; Zhu, X.; Zhu, J.; Cheng, Z.; Zhang, W. *Polymer* **2005**, *46*, 12716.

(18) Luan, Z.; Fournier, J. A.; Wooten, J. B.; Miser, D. E. *Microporous Mesoporous Mater.* **2005**, *83*, 150.

(19) van Berkel, P. M.; Driessen, W. L.; Reedijk, J.; Sherrington, D. C. *Chem. Commun.* **1995**, 147.